Series AC Arc Fault Detection
Using Only Voltage Waveforms

Jonathan C. Kim*, Dorin O. Neacşu*, Brad Lehman*
Department of Electrical and Computer Engineering
Northeastern University
Boston, MA, USA
kim.jonat@husky.neu.edu

Roy Ball
MERSEN USA Newburyport-MA, LLC
Newburyport, MA, USA

Abstract—**This research generates series AC arc faults and then detects them using voltage waveforms instead of the traditional current waveforms. The detection algorithm analyzes a unique symmetric energy profile generated by the arc fault. The experimental results demonstrate that the harmonics generated by an arc fault's ignition and extinction can be sensed by voltage measurements at the voltage source where the arc fault circuit interrupters (AFCI) are located.**

Keywords—series arc faults, symmetric energy profile, threshold violation rule

I. INTRODUCTION

One of the leading causes of electrical fires in residential homes is AC arc faults [1]. Therefore, the National Electrical Code (NEC) now requires that all 120 V, single-phase, 15 A and 20 A branch circuits supplying outlets installed in kitchens, family rooms, dining rooms, living rooms, bedrooms, hallways, laundry areas, etc. must be protected by arc fault circuit interrupters (AFCI) [2]. The purpose of an AFCI is to de-energize a sustained electric arc to prevent fires. Consequently, AFCI are different from ground fault circuit interrupters (GFCI), which de-energize the circuit to prevent a person from receiving a potentially fatal shock. The International Standard (IEC 62606) and UL 1699 outline general requirements to test the performance of an AFCI to detect arc faults and avoid unwanted tripping scenarios [3]-[4].

Several AC arc fault models and detection methods have been developed with additional recommendations for performance testing to determine the AFCI's compatibility with noisy home electrical products [5]-[7]. Traditional AFCI and AC arc fault detection models are based on time and frequency analysis of the current measurement using either short-time Fourier Transform (STFT) or Discrete Wavelet Transforms (DWT) [8]-[10]. They observe changes in the harmonic component and use pre-determined thresholds to distinguish arc fault noise from electronic devices that produce noise similar to arc faults. However, STFT and DWT methods by themselves depend on properties and features of the sensed line currents that are not unique to arc faults [8]-[10]. Also, they require multi-level filtering that may increase the computation time for determining an arc fault. Another algorithm [11] observes the chaotic behavior of the current during an arc fault and uses quantum probability model theory to calculate the current entropy.

Other proposed methods in [12]-[14] combine frequency analysis with neural networks or classification with support vector machines (SVM) to increase the accuracy of detection. A Kalman filtering algorithm also exists which monitors the deviation of the eigenvalue of each power cycle to determine an arc fault [15]. However, these detection rules require the training of large number of arc fault samples to generate a feature space using eigenvectors [12]-[14]. If electrical devices similar to arc faults have not been tested in the development process of an AFCI, unwanted tripping scenarios may occur. Thresholds for time-frequency dependent algorithms and the feature space in machine learning strategies will need to be adjusted accordingly to include these devices.

To overcome these limitations, this paper proposes a new series AC arc fault detection method for AFCI using the voltage waveform and a symmetric energy profile that is exclusive to arc faults. AC arc faults have an ignition and extinguishing cycle that generate two discontinuities per cycle around the zero-crossing. In summary, this paper presents the following research contributions:

1) Unlike traditional arc fault detection approaches, the voltage waveform is utilized to extract a symmetric energy profile exclusive to the arc fault for analysis, distinguishing it from loads that otherwise show arc fault behaviors in the current waveform.

2) The arc fault detection algorithm relies on a set of threshold violation rules which does not use non-stationary signal analysis or machine learning techniques.

This paper will proceed as follows: Section II briefly introduces the characteristics of an arc fault and experimental setup of the arc fault generator; Section III outlines the series AC arc fault detection algorithm; Section IV discusses the experimental results; and Section V concludes the paper.

II. EXPERIMENTAL SETUP OF ARC FAULT GENERATOR

A. Generating an AC Arc Fault

An arc fault forms when a high electric potential between two conductors (above the breakdown voltage) causes the air to become conductive. The average breakdown voltage is between 25 kV/cm to 30 kV/cm [16] and is dependent on the insulating material, the shape of the conductor tip and the gap distance between the two conductors.
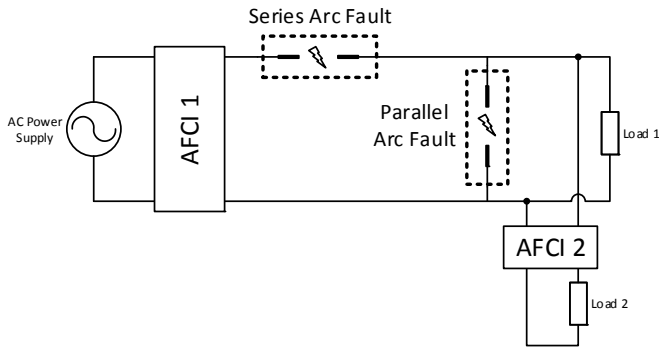
Fig. 1. Series and parallel arc faults. AFCI 2 will de-energize power to load 2 but is unable to shutdown power to the series arc fault.
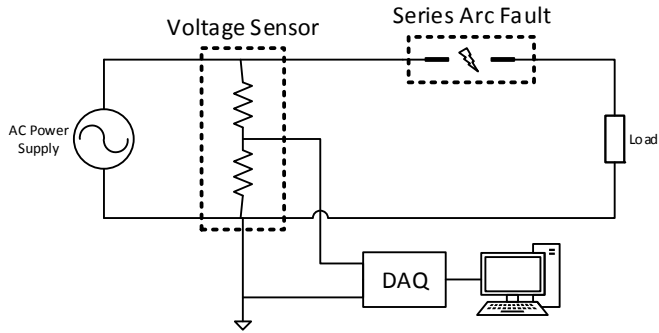

Fig. 2. Schematic diagram of the experimental setup

There are two categories of AC arc faults: parallel and series. Parallel arc faults occur between two distinct active conductors or from an active conductor to ground as seen in Fig. 1 [2]. Series arc faults occur when there is a break in the electrical path of an active conductor as seen in Fig. 1 [2]. Series AC arc faults are more common and are often caused by loose terminals or degradation of wires and connectors. The series arc faults are current limited by the load and are able to sustain arc faults undetected by overcurrent devices and some AFCI. Therefore, series arc faults are considered more dangerous than parallel arc faults.

B. Hardware Setup

A series AC arc fault generator has been set up according to the schematic diagram shown in Fig. 2. A photograph of the experimental equipment and setup is shown in Fig. 3. The voltage source is a sinusoidal signal generated by a programmable AC source (Chroma 61504) and is later replaced directly by the grid. A voltage divider made of two resistors in series is placed parallel to the voltage source to downscale the voltage to within a range of -10 V to +10 V. The measured voltage signal is sampled using the data acquisition device by National Instruments (USB-6341) and analyzed by the arc fault detection algorithm in MATLAB. The arc gap is created using two solid non-melting carbon alloys in a dust tight transparent enclosure. The loads tested were power resistors. The main parameters of each component are given in Table I.

The voltage across the arc gap and the load is not measured because in real applications the exact location of the arc fault is unknown. For example, an AFCI (AFCI 2) is placed near the load, as shown in Fig. 1. If a series arc fault occurs behind the outlet, in the insulation of the house as shown, AFCI 2 will be
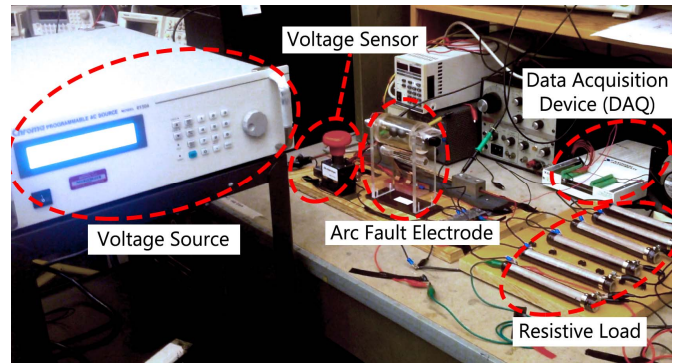

Fig. 3. Photograph of experimental equipment and setup

able to detect the frequency changes on the line and de-energize the circuit. However, the series arc fault is still energized and will cause an undetected fire. Therefore, in this research, the voltage is measured at the source, which is equivalent to the AFCI being placed at the circuit breaker panel to monitor the noise of circuit.

C. Arc Fault Voltage

Although the location and exact shape of the arc fault voltage signal is unknown during an actual event, a typical voltage waveform, given in Fig. 4(a), is analyzed to understand how the arc fault affects the voltage source. As the source voltage rises, the voltage drop across the arc gap also increases as seen in section (*1*) of the plot. After the arc gap voltage reaches the breakdown voltage, the arc ignites. The arc fault acts like a small resistor. Therefore, the impedance across the arc gap is no longer very large. This causes the arc gap voltage to drop and remain relatively constant as seen in section (*2*) of the waveform. A minimum voltage is needed to sustain the arc across the constant arc gap. Therefore, as the source voltage begins to pass through the zero-crossing, the arc fault will extinguish itself. The arc gap impedance will become very large and the arc gap voltage will follow the source voltage as seen in section (*3*) of the measured signal. During this time, the magnitude of the current is zero and is often referred to as the "current shoulder" as seen in Fig. 4(b) [7]-[10]. As the magnitude of the source voltage rises again, the voltage drop across the arc gap exceeds the breakdown voltage and reignites the arc for the negative cycle as shown in section (*4*) of the signal in Fig. 4(a).

TABLE I
ARC FAULT GENERATOR PARAMETERS

| Equipment	Model	Parameter Settings
Voltage Source	Chroma 61504 / Grid	120 Vrms, 60 Hz
Resistive Load	-	5 power resistors: 100 Ω each All in parallel: 20 Ω Power consumption: 1.44 kW
Electrodes	SG40-H	Solid non-melting carbon alloy 2 kV-40 kV tolerance 1" diameter Arc gap accuracy ±2%
Data Acquisition Device	NI-USB-6341	Sampling frequency: 500 ksps Total sample time: 1 s Voltage input range: ±10 V
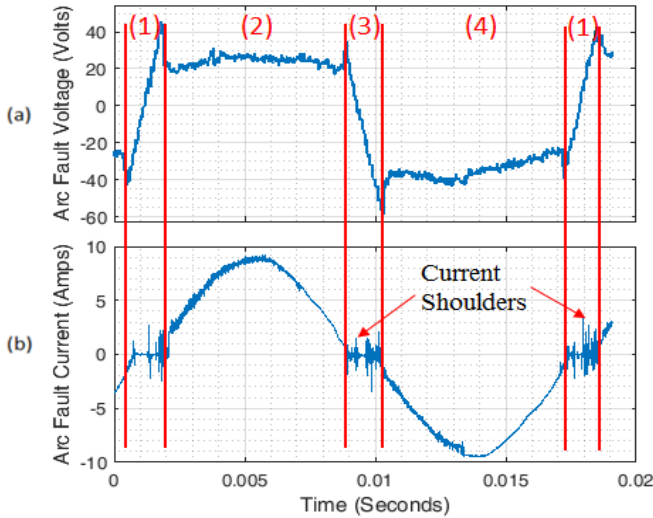
Fig. 4. A typical experimentally measured voltage waveform across the arc gap. Section (1) and (3) represented extinguished periods and section (2) and (4) represent arc ignition periods.
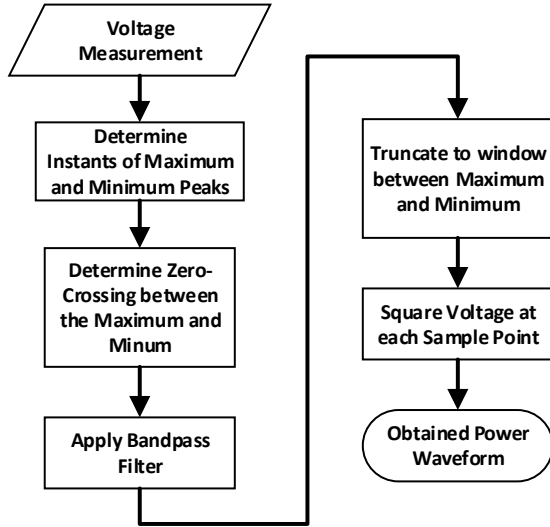

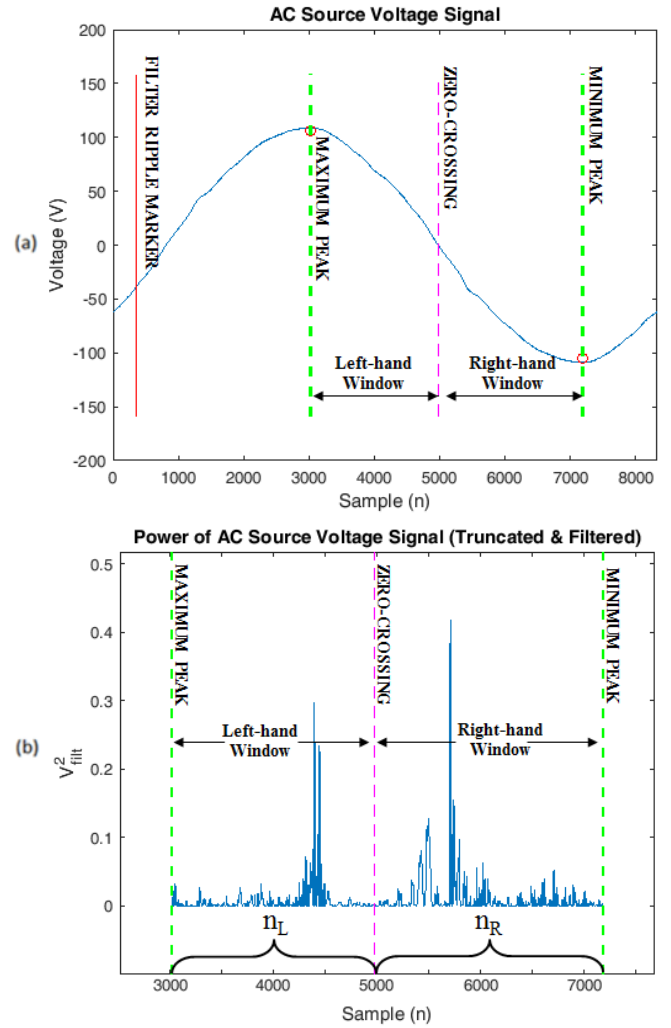Fig. 5. Algorithm for obtaining the power of the voltage signal at each time instant.

Fig. 6. Location of left-hand and right-hand measurement window markers and calculation of the power waveform from the voltage signal of an arc fault.

III. SERIES AC ARC FAULT DETECTION ALGORITHM

The new AC arc fault detection algorithm relies on the ignition and extinction transients of the arc fault around the zero-crossing that produce a unique symmetric energy profile. When this symmetric energy profile is observed over a fixed number of cycles, an arc fault is declared.

A. Obtaining Power Waveforms

A power waveform is calculated from the voltage measurement to prepare for the extraction of five distinct energy signals. A flow chart is given in Fig. 5. The voltage measurement observes a single 60Hz voltage cycle at the sampling frequency of 500 kHz. The voltage cycle is then split into two measurement windows: one window spans the time from the maximum peak occurrence of the voltage cycle to the time of the zero-crossing and the second window spans the time of the zero-crossing to the minimum peak of the voltage cycle as shown in Fig. 6(a).

After the markers for each window are placed, the voltage signal is passed through the band-pass filter. All data outside the measurement window is removed and the remaining filtered voltage signal is split into the left-hand and right-hand measurement windows, $V_{filt,L}$ and $V_{filt,R}$, respectively. The filtered voltage signal is squared at each sample point to produce the power waveform. The result is a power waveform, V_{filt}^2, with markers that divide the waveform into a left-hand and right-hand power waveform window as shown in Fig. 6(b).

B. Energy Calculation

From the prepared power waveform, five distinct energy signals are calculated: 1) two instantaneous energy signals, 2) two differential energy signals, and 3) a symmetric energy signal. There are two instantaneous and differential energy signals each because one energy signal is calculated for each measurement window, a left-hand energy and right-hand energy signal. There is only one symmetric energy signal because it is a comparison of energy between both measurement windows.
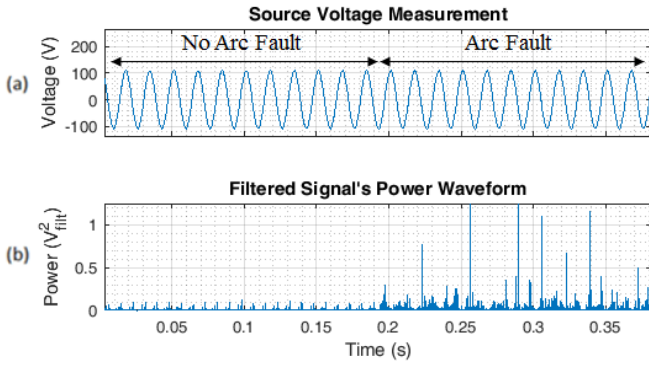
Fig. 7. A filtered source voltage's power waveform where the arc fault is initiated at 0.194 s.
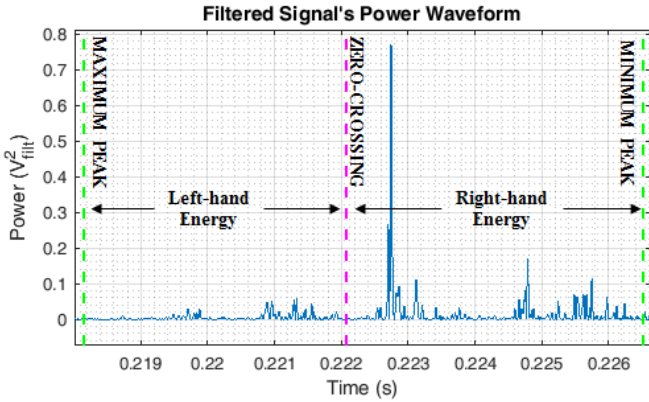

Fig. 8. An intermittent violent ignition, skewed series arc fault power waveform.

The left-hand instantaneous energy (E_L) and right-hand instantaneous energy signal (E_R) is generated by the summation of all the power samples in the left-hand and right-hand measurement windows, respectively as calculated in (1). The left-hand differential energy (ΔE_L) and differential right-hand (ΔE_R) is generated by taking the absolute difference between the present left-hand and right-hand instantaneous energy and the previous left-hand and right-hand instantaneous as calculated in (2). Lastly, the symmetric energy (E_{sym}) is generated by taking the absolute difference between the present left-hand instantaneous and right-hand instantaneous energy as calculated in (3). The equations are given below where "k" is each measurement cycle and "n" is the sampled time of each cycle:

$$E_L[k] = \sum V^2_{filt,L}[n] \ \& \ E_R[k] = \sum V^2_{filt,R}[n] \quad (1)$$
$$\Delta E_L[k] = |E_L[k] - E_L[k-1]| \quad (2a)$$
$$\Delta E_R[k] = |E_R[k] - E_R[k-1]| \quad (2b)$$
$$E_{sym}[k] = |E_L[k] - E_R[k]| \quad (3)$$

The following three threshold conditions are met for the arc fault to be detected:

$$E_L[k] > noise_{thresh} \quad OR \quad E_R[k] > noise_{thresh} \quad (4)$$
$$\Delta E_L[k] > var_{thresh} \quad OR \quad \Delta E_R[k] > var_{thresh} \quad (5)$$
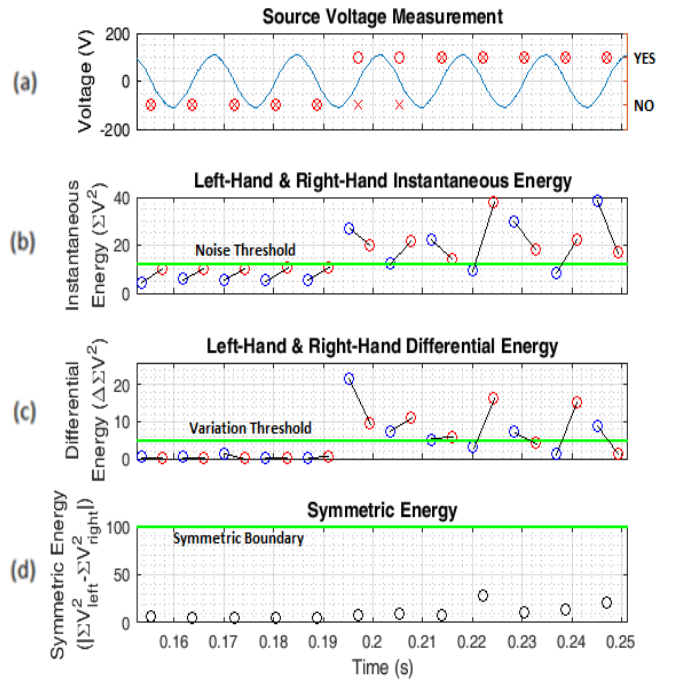$$E_{sym}[k] < sym_{bound} \quad (6)$$

Fig. 9. Experimental result: (a) Source voltage measurement with potential arc fault alerts (red 'o') and arc fault detection flags (red 'x'); (b) Left-hand (blue) and right-hand (red) instantaneous energy with a noise threshold (green); (c) Left-hand (blue) and right-hand (red) differential energy with a variation threshold (green); (d) Symmetric energy (black) and the symmetric boundary (green).

When all (4), (5), and (6) are true for at least three consecutive cycles, (k, k+1, k+2), an arc fault is declared. The noise threshold detects increase in the overall noise related to the increase in the magnitude of the frequency response. The variation threshold detects the fluctuations in the instantaneous energy, observed through the differential energy, related to the fluctuations in the arc fault impedance. The symmetry boundary tracks the symmetric energy profile. Using properties of the symmetric energy helps reduce false alarms often generated by electronic loads.

IV. EXPERIMENTAL RESULTS

A. Analysis of Power Waveform

In Fig. 7, an arc fault is initiated at 0.194 s in series with a 1.44 kW load. In Fig. 7(b), before the arc fault the magnitude of the power waveform, V_{filt}^2, is consistent near zero. After the arc fault is initiated, the overall magnitude of the power waveform increases by around 525%. The peak power before and after the arc fault sees an increase of almost 700%.

Each power waveform window shows two peaks, one on either side of the zero-crossing as shown in Fig. 6(b). However, as the arc fault continues to burn, the ignition stage may intermittently be more violent as the plasma forms across ions that were generated from the previous arcing stages. There are intermittent moments, as shown in Fig. 8, where the power of the ignition (in this case the right-hand energy window) is greater than that of the extinction (left-hand energy window). Therefore, the symmetric energy is not always close to zero and

the boundary is set to take into account the intermittent high energy spikes.

B. Analysis of Energy Profiles

The energy characteristics of the series arc fault scenario seen in Fig. 7 is shown in Fig. 9. In the energy plots, Fig. 9(b) and Fig. 9(c), the green line in each of the energy plots are the threshold conditions for each respective energy signal, the left-hand (blue) and right-hand (red) energy signals are paired by a black line. The symmetric energy (black) in Fig. 9(d) is compared against the symmetric boundary (green). In Fig. 9(a), the potential arc fault flags (red 'o') and arc fault detection flags (red 'x') are given with the voltage measurement.

The arc fault is initiated at 0.194 s, a potential arc fault is declared after 4 ms and detected by 0.214 s. In total, the interrupt signal to de-energize the circuit is after the arc fault is initiated is 20ms. This is the fastest time the algorithm can detect the arc fault.

V. CONCLUSION

This paper introduces a new method for detecting series AC arc faults using voltage measurements instead of the traditional current measurement approach. A symmetric energy profile corresponding to the ignition and extinction characteristics of the arc fault is observed in the voltage measurement at the circuit breaker panel. The detection algorithm is a set of three threshold violation rules and does not need any previously acquired large data sets for classification methods involving machine learning techniques. The experimental results show that a series arc fault can be detected within two voltage cycles.

REFERENCES

[1] USFA, 2015. *Residential and nonresidential building fire and fire loss estimates by property use and cause (2003-2015).* United States Fire Administration, https://www.usfa.fema.gov/data/statistics/order_download_data.html#download

[2] National Electrical Code, 2017 Edition, NFPA70, National Fire Protection Association, Batterymarch, MA.

[3] *International Standard: General requirements for arc fault detection devices,* IEC 62606, 2013.

[4] Underwriter Laboratories Inc., *UL Standard for Safety: Arc-Fault Circuit-Interrupters*, UL 1699, Third Edition, May 3, 2017.

[5] "Recommendations on AFCI home electrical product compatibility," NEMA, Rosslyn, VA, USA, ABP 2, 2011. [Online]. Available: https://www.hbag.org/uploads/5/7/9/1/57910935/recommendations_on_afci___home_electrical_product_compatibililty.pdf

[6] G. D. Gregory and G. W. Scott, "The arc-fault circuit interrupter, an emerging product," *1998 IEEE Industrial and Commercial Power Systems Technical Conference. Conference Record. Papers Presented at the 1998 Annual Meeting (Cat. No.98CH36202)*, Edmonton, Alta., 1998, pp. 48-55.

[7] G. Artale, A. Cataliotti, V. Cosentino and G. Privitera, "Experimental characterization of series arc faults in AC and DC electrical circuits," *2014 IEEE International Instrumentation and Measurement Technology Conference (I2MTC) Proceedings*, Montevideo, 2014, pp. 1015-1020.

[8] H. Cheng, X. Chen, F. Liu and C. Wang, "Series Arc Fault Detection and Implementation Based on the Short-time Fourier Transform," *2010 Asia-Pacific Power and Energy Engineering Conference*, Chengdu, 2010, pp. 1-4.

[9] W. Chi-Jui, L. Yu-Wei, "Smart detection technology of serial arc fault on low-voltage indoor power lines," *International Journal of Electrical Power & Energy Systems*, vol. 69, pp. 391-398, July 2015.

[10] K. Koziy, B. Gou and J. Aslakson, "A Low-Cost Power-Quality Meter With Series Arc-Fault Detection Capability for Smart Grid," in *IEEE Transactions on Power Delivery*, vol. 28, no. 3, pp. 1584-1591, July 2013.

[11] N. L. Georgijevic, M. V. Jankovic, S. Srdic and Z. Radakovic, "The Detection of Series Arc Fault in Photovoltaic Systems Based on the Arc Current Entropy," in *IEEE Transactions on Power Electronics*, vol. 31, no. 8, pp. 5917-5930, Aug. 2016.

[12] Yang, Kai et al. "A Novel Arc Fault Detector for Early Detection of Electrical Fires." Ed. Ingolf Willms. *Sensors (Basel, Switzerland)* 16.4 (2016): 500. *PMC*. Web. 12 June 2018.

[13] W. Chi-Jui, L. Yu-Wei, H. Chen-Shung, "Intelligent Detection of Serial Arc Fault on Low Voltage Power Lines," *Journal of Marine Science and Technology*, vol. 25, no. 1, pp. 43-53, 2017.

[14] Kai Yang, Rencheng Zhang, Shouhong Chen, Fujiang Zhang, Jianhong Yang, Xingbin Zhang, "Series Arc Fault Detection Algorithm Based on Autoregressive Bispectrum Analysis", *Algorithms*, vol. 8, pp. 929, 2015, ISSN 1999-4893.

[15] S. Zhang, F. Zhang, P. Liu, Z. Han, "Identification of Low Voltage AC Series Arc Faults by using Kalman Filtering Algorithm," *Elektronika ir Elektrotechnika*, vol. 20, no. 5, pp. 51-56, 2014

[16] J. Johnson, K. M. Armijo, M. Avrutsky, D. Eizips and S. Kondrashov, "Arc-fault unwanted tripping survey with UL 1699B-listed products," *2015 IEEE 42nd Photovoltaic Specialist Conference (PVSC)*, New Orleans, LA, 2015, pp. 1-6.

[17] A. D. Stokes, W. T. Oppenlander, "Electric arcs in open air," in *Journal of Physics D: Applied Physics*, vol. 24, no. 1, pp. 26-35, 1991.

[18] J. Andrea, P. Schweitzer and E. Tisserand, "A New DC and AC Arc Fault Electrical Model," *2010 Proceedings of the 56th IEEE Holm Conference on Electrical Contacts*, Charleston, SC, 2010, pp. 1-6.

[19] P. Qi, J. Lezama, S. Jovanovic and P. Schweitzer, "Adaptive real-time DWT-based method for arc fault detection," *ICEC 2014; The 27th International Conference on Electrical Contacts*, Dresden, Germany, 2014, pp. 1-6.

[20] W. Zhan, S. McConnell, R. S. Balog, J. Johnson, "Arc fault signal detection—Fourier transformation vs. wavelet decomposition techniques using synthesized data", *Proc. IEEE 40th Photovolt. Spec. Conf. (PVSC)*, pp. 3239-3244, 2014.

[21] C. Parameswariah and M. Cox, "Frequency Characteristics of Wavelets," in *IEEE Power Engineering Review*, vol. 22, no. 1, pp. 72-72, Jan. 2002.

[22] Y. H. Gu and M. H. J. Bollen, "Time-frequency and time-scale domain analysis of voltage disturbances," in *IEEE Transactions on Power Delivery*, vol. 15, no. 4, pp. 1279-1284, Oct. 2000.